



**PECS VIII ~ The 8th International Photonic & Electromagnetic  
Crystal Structures Meeting**

Postdeadline Session

Thursday April 9, 2009

Chair: Yuri Kivshar

**Program:**

*2:30-2:40 - Student prizes*

*2:40-3:42 - Postdeadline papers (10 mins + 2 mins questions)*

*2:40 - Suppression of radiation loss by hybridization effect in  
two coupled split-ring resonators*

H. Liu, T. Q. Li, T. Li, Z. G. Dong, S. M. Wang, S. N. Zhu,  
and X. Zhang

*2:52 - Extremely large free spectral range (>300 nm) filter based  
on photonic crystal vertical directional coupler*

M. Grande, L. O'Faolain, T. P. White, M. Spurny, A. D'Orazio  
and T. F. Krauss

*3:04 - A two-dimensional nonlinear electric metamaterial*

D. A. Powell, I. V. Shadrivov, and Yu. S. Kivshar

*3:18 - Hyperlens formed by array of metallic rods*

P.A. Belov, G. Palikaras, Y. Zhao and C. Simovski

*3:30 - Soliton Mediated Optical Quantization in Bragg Gratings*

Falk Eilenberger, C. Martijn de Sterke, and Benjamin J. Eggleton

# Suppression of radiation loss by hybridization effect in two coupled split-ring resonators

H. Liu<sup>1,\*</sup>, T. Q. Li<sup>1</sup>, T. Li<sup>1</sup>, Z. G. Dong<sup>1</sup>, S. M. Wang<sup>1</sup>, S. N. Zhu<sup>1</sup>, X. Zhang<sup>2</sup>

<sup>1</sup> Department of Physics, Nanjing University, Nanjing, Jiangsu, P. R. China,

<sup>2</sup> Nanoscale Science and Engineering Center, University of California, 5130 Etcheverry Hall, Berkeley, California 94720-1740, USA

Email: [liuhui@nju.edu.cn](mailto:liuhui@nju.edu.cn); URL: <http://dsl.nju.edu.cn/dslweb/images/plasmonics-MPP.htm>

Magnetic metamaterial research has attracted significant interest since Pendry reported that split ring resonators (SRR) - nonmagnetic metallic structures with sizes below the diffraction limit - can exhibit negative permeability [1]. The effective medium composed of SRRs can support resonant magnetic plasmon (MP) oscillation analogous to surface plasmon resonance. Combined with negative permittivity material at the same response frequency region, a negative refraction effect was produced, leading to a wealth of research into metamaterials. In addition to negative refraction, Pendry also proposed that SRRs could be used to enhance nonlinear optical phenomena [1]. In recent years, some groups have begun to apply magnetic resonance nanostructures to nonlinear optical effects such as SHG, nanolaser, and SPASER. Since all of these nonlinear processes are based on resonance behavior, a high quality factor (Q-factor) was pursued to render the magnetic plasmon structures more efficient. Methods were introduced to improve the resonance properties of magnetic structures - for example, weakly asymmetric structures that enable the excitation of trapped modes. However, due to dramatic radiation loss caused by strong coupling to free space, the Q-factor of magnetic resonators is still quite low. Accordingly, the inhibition of radiation loss is necessary to obtain high Q magnetic nanocavities.

Although metamaterials possess many interesting applications, the coupling interactions between the elements in metamaterials are somewhat ignored by most of researchers in this field; therefore, the effective properties of metamaterials can be viewed as the “averaged effect” of the resonance property of the individual elements. However, the coupling interaction between elements should always exist when they are arranged together into real practical metamaterials. Sometimes, especially when the elements are very close, this coupling effect is not negligible and will have a substantial effect on the metamaterial’s properties.

Recently, our group devised a new type of magnetic resonance structure, the magnetic dimer (MD), which is composed of two coupled SRRs. Strong magnetic coupling interaction is established between the two SRRs and it introduces two hybrid magnetic plasmon modes - a lower frequency bonding mode, and a higher frequency antibonding mode [2]. Optical activity was experimentally observed in this MD system, which results from this hybridization effect [3]. Besides, this type of MD structure was also recently reported to construct stereometamaterials with different twisted angles [4].

In our recent submitted paper [submitted to *Phys. Rev. B*, (2009)], we analyze the radiation properties of the coupled MD structure in the THz region, where simultaneous magnetic and electric couplings coexist. By researching the far field radiation of this structure, we observed two different radiation patterns in these two hybrid modes due to different resonant behaviors. Compared with the single split ring resonator, we found that the radiation loss was greatly suppressed at the lower symmetry mode, resulting in a dramatic increase in the Q-factor of this structure. Moreover, the Q-factor changed continuously with the variation in the distance between the two SRRs. This leads to a possible design for a nanocavity with an adjustable Q-factor.

## References

- <sup>1</sup> J. B. Pendry, A. J. Holden, D. J. Robbins, and W. J. Stewart, *IEEE Trans. Microwave Theory Tech.* **47**, 2075 (1999).
- <sup>2</sup> H. Liu, D. A. Genov, D. M. Wu, Y. M. Liu, Z. W. Liu, C. Sun, S. N. Zhu, and X. Zhang, *Phys. Rev. B* **76**, 073101 (2007)
- <sup>3</sup> T. Q. Li, H. Liu, T. Li, S. M. Wang, F. M. Wang, R. X. Wu, P. Chen, S. N. Zhu and X. Zhang, *Appl. Phys. Lett.* **92**,131111 (2008)
- <sup>4</sup> N. Liu, H. Liu, S. N. Zhu and H. Giessen, *Nature Photonics* **3**,157 (2009).

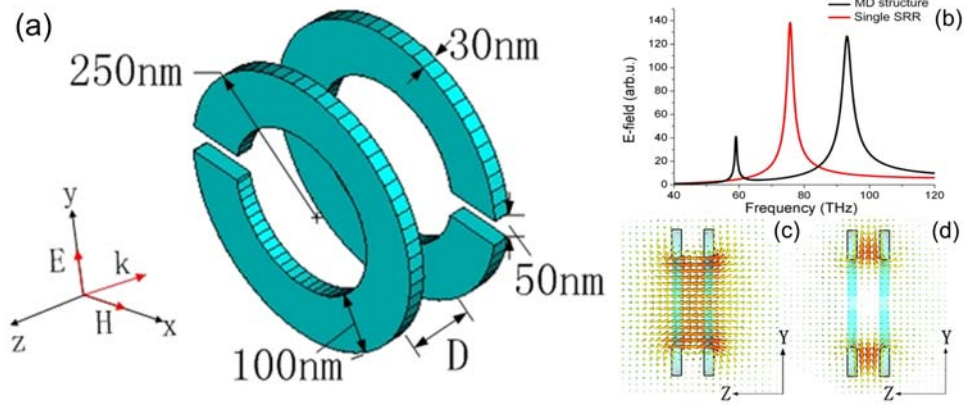


Figure 1 (a) Structure of the MD structure; (b) Transmission of a single SRR structure (Red curve) and a MD structure (Black curve). Local magnetic field distribution at bonding mode (c) and antibonding mode (c) in  $y$ - $x$  plane.

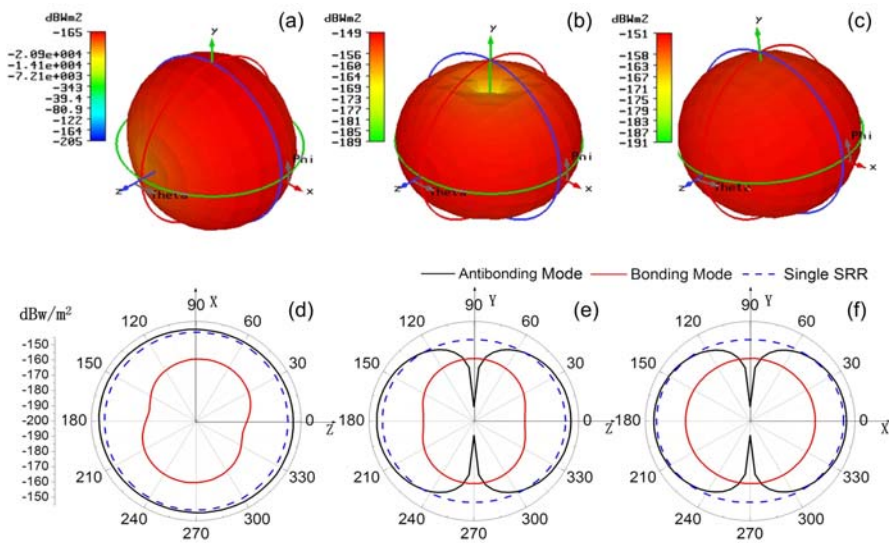


Figure 2 The logarithmic radiation skin: (a) bonding mode of MD, (b) antibonding mode of MD, and (c) the single SRR. The distance between two SRRs is set as  $D=140\text{nm}$ ; The projection of the 3D radiation skin in (d)  $x$ - $z$  plane, (e)  $y$ - $z$  plane and (f)  $x$ - $y$  plane. The distance between two SRRs is set as  $D=140\text{nm}$ .

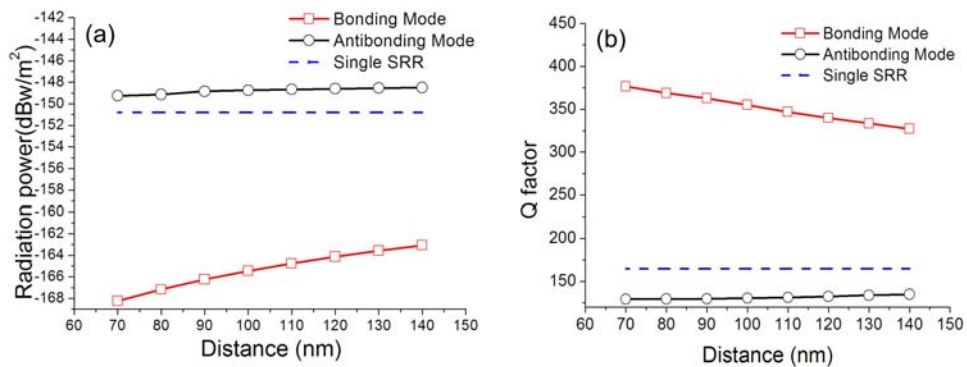


Figure 3 (a) Radiation power under different distances; (b)  $Q$ -factors under different distances. (red line: bonding mode of MD; black line: antibonding mode of MD; blue dash line: the single SRR)

# Extremely large free spectral range (>300 nm) filter based on photonic crystal vertical directional coupler

M. Grande<sup>1,2</sup>, L. O'Faolain<sup>1</sup>, T. P. White<sup>1</sup>, M. Spurny<sup>1</sup>, A. D'Orazio<sup>2</sup>, T. F. Krauss<sup>1</sup>

<sup>1</sup>*School of Physics and Astronomy, University of St Andrews, St Andrews, Fife, KY169SS, UK*  
mg81@st-andrews.ac.uk, jww1@st-andrews.ac.uk, tom.white@st-andrews.ac.uk, tfk@st-andrews.ac.uk

<sup>2</sup>*DEE, Politecnico di Bari, Via Re David 200, 70125, Bari, Italy*  
dorazio@poliba.it

Optical filters are a key building block for wavelength division multiplexing (WDM) applications. A number of schemes already exist to realise this multiplexing function, such as arrayed waveguide gratings (AWGs), microring resonators and coupled-ring resonator systems. Most of these fall short when a wide free spectral range (FSR) is required, as in the combined L-C optical telecommunication bands ( $\Delta\lambda \sim 100$  nm), in sensing or in astrophotonics applications. A widely used filter is the microring resonator, with the highest FSR of 47 nm reported to date, using a ring radius of 2  $\mu\text{m}$  [1]. The FSR is limited by the size of the microring and bending losses would increase sharply if the device were made even smaller to achieve a higher FSR.

Photonic crystals (PhCs) offer new possibilities for ultra compact wavelength selective optical devices owing to their confinement and dispersive properties. Even so, filters based on the popular L3 photonic crystal cavity also suffer from a low (10's of nm) FSR [2]. In this paper, we demonstrate the combination of a slow light photonic crystal waveguide with a polymer waveguide for the fabrication of a directional coupler based filter with a free spectral range exceeding  $\Delta\lambda > 300$  nm.

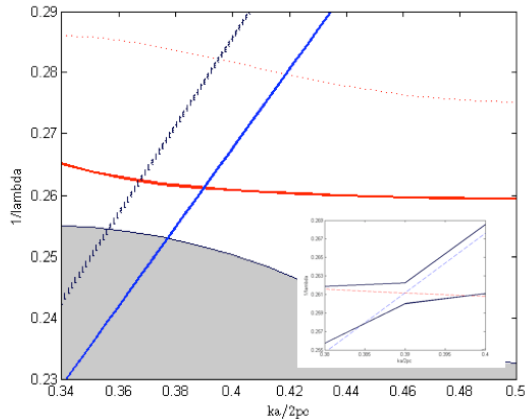


**Fig. 1:** 3-D calculated band structure: silica lightline (dashed line), polymer waveguide (blue line), W1 waveguide (red line), odd defect mode (dotted line); inset: anticrossing point (enlarged).

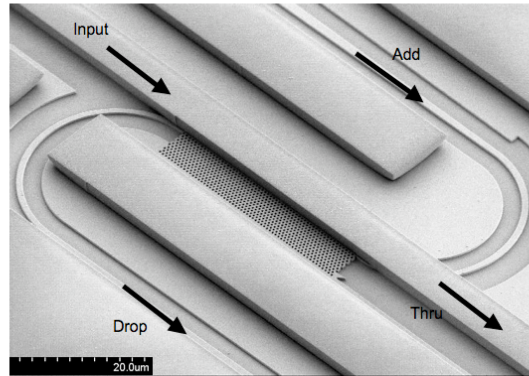


**Fig. 2:** Micrograph of the fabricated device (the FOx layer has been removed for clarity).

In a two-waveguide coupled system, coupling occurs when the two wavevectors coincide [3-5]. Figure 1 depicts the dispersion curve of the photonic crystal waveguide superimposed on the polymer ridge waveguide. It is worthwhile to point out that the two waveguides have largely different group velocities, which, in fact, is the reason for the narrow bandwidth of the filter. The mini-stop band that arises at the anticrossing point forces the input signal to be coupled into a backward propagating mode, so the modes propagating in the polymer and the PhC waveguide, respectively, are counterpropagating.

To verify the simulation results, we fabricated the device from an SOI wafer comprising a nominally 220 nm thick silicon layer on 2  $\mu\text{m}$  of silica. The photonic crystal was fabricated by means of electron beam lithography with ZEP-520A resist as described in [6, 7]. The sample was then covered by a layer of FOx-14 (Flowable Oxide, Dow Corning) by spin coating after the resist removal. The FOx

penetrates the holes of the photonic crystal effectively as demonstrated in [7]. The polymer waveguide is obtained by using 2 layers of ZEP and a second electron beam exposure with a 3-point alignment procedure using pre-existing markers. Fig. 2 shows the final device without the intermediate FOx layer.

A supercontinuum source (Koheras Super-K Compact) was used to characterize the device in the wavelength range from 1300 nm to 1650 nm. The fabricated devices were realised with and without the FOx layer, lengths of 40  $\mu\text{m}$  and 60  $\mu\text{m}$  and lattice periods of 420 nm and 410 nm, respectively. The measurements show that maximum coupling occurs at wavelengths of 1587 nm and 1575 nm, respectively (Fig 3). The polymer waveguide mode also couples with the continuum of modes in the dielectric band (for wavelengths  $>1625$  nm) but the coupling is negligible elsewhere. Thus the free spectral range (FSR) can be considered equal to the distance of the crossing point between the polymer dispersion curve and the air and dielectric bands, i.e. of order of the photonic bandgap. The measurements show a FSR of more than 300 nm with a fullwidth half maximum (FWHM) of 2.5 nm and 1.9 nm respectively, and a sidelobe suppression ratio (SLSR) of about 16 dB. The device shows also another important feature: high efficiency coupling of light between a polymer waveguide and a PhC waveguide, which at first sight is surprising, given that the material indices are so different.

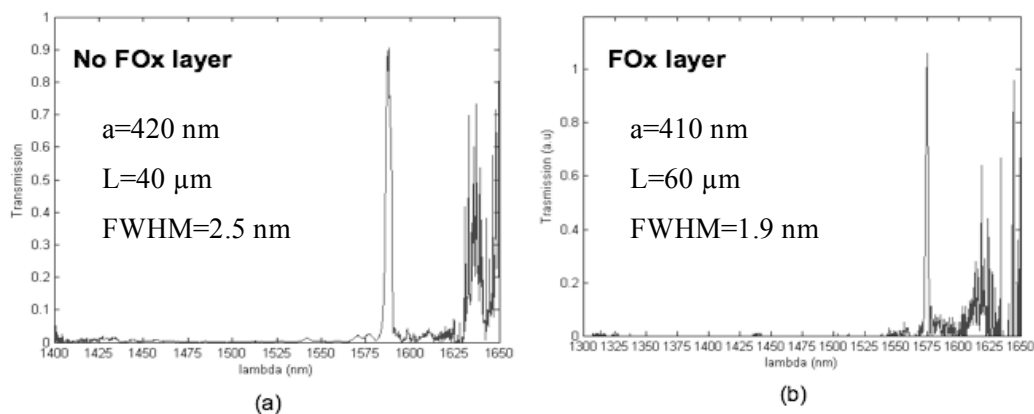


**Fig. 3:** Measured filter response at the drop port without (a) and with (b) the FOx layer respectively.

In conclusion, we have demonstrated a new type of slow-light enhanced filter that may be used as the basic element of an on-chip spectrometer with nanometer wavelength resolution. Tailoring the slow light properties of the photonic crystal waveguides offers the potential for further enhancements in terms of filter response (e.g. achieving a “flat-top”), sidelobe suppression, as well as tunability, e.g. via localised heating. Multiple filters can be cascaded for a multichannel device. The device does not require a spot size converter or inverse taper, allowing the input signal from an external optical fibre to be coupled directly into the polymer waveguide. The extremely large FSR ( $>300$ nm) overcomes one of the major bottlenecks of existing filters.

## References

- [1] M. S. Nawrocka, T. Liu, X. Wang, R. R. Panepucci, Applied Physics Letters, 89, 071110 (2006).
- [2] A. R. A. Chalcraft, S. Lam, D. O’Brien, T. F. Krauss, M. Sahin, D. Szymanski, D. Sanvitto, R. Oulton, M. S. Skolnick, A. M. Fox, D. M. Whittaker, H.-Y. Liu and M. Hopkinson, Appl. Phys. Lett. 90, 241117 (2007).
- [3] P. E. Barclay, K. Srinivasan, O. Painter, J. Opt. Soc. Am. B, 20, 2274-2284 (2003).
- [4] C. Grillet, C. Smith, D. Freeman, S. Madden, B. Luther-Davies, E. Magi, D. Moss, and B. Eggleton, Opt. Express 14, 1070-1078 (2006).
- [5] Z. Zhang, U. Andersson, M. Qiu, Active and Passive Electronic Components, Volume 2007 (2007).
- [6] L. O’Faolain, X. Yuan, D. McIntyre, S. Thoms, H. Chong, R. M. De la Rue, and T. F. Krauss, Electron. Lett. 42, 1454-1455 (2006).
- [7] T. P. White, L. O’Faolain, Juntao Li, L. C. Andreani, and T. F. Krauss, Opt. Express 16, 17076-17081 (2008).

## A two-dimensional nonlinear electric metamaterial

D. A. Powell, I. V. Shadrivov, and Yu. S. Kivshar

*Nonlinear Physics Centre,  
Research School of Physics and Engineering,  
Australian National University,  
Canberra ACT 0200, Australia  
email: david.a.powell@anu.edu.au*

We design and study nonlinear electric metamaterials operating at microwave frequencies. By introducing a varactor diode as a nonlinear element in each electric oscillator, we are able to shift the location of the negative permittivity stop-band by changing the incident power. These elements could be combined with the previously developed nonlinear magnetic metamaterials in order to create negative index media with both electric and magnetic nonlinearities.

Negative index metamaterials are typically fabricated from structures exhibiting both negative electric and magnetic responses. Split-ring resonators are the best known elements of structures with a negative magnetic response, and arrays of long wires are commonly used to create a negative electric permittivity [1]. However, such large-scale structures are unsuitable for many applications, such as transform optics which require local variations in the unit cell parameters and which may require a non-tetragonal cell symmetry. One of the solutions to this problem is the use of electric resonators constructed from two resonant loops having a fundamental mode whereby the total magnetic dipole moment is canceled out, leaving a nonvanishing electric dipole moment [2, 3].

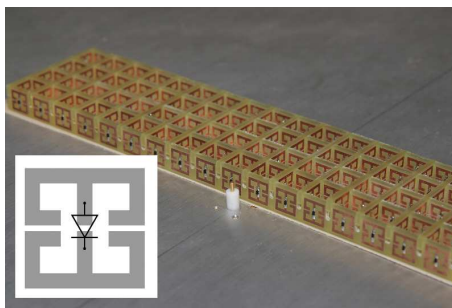


FIG. 1: Slab of nonlinear electric metamaterials with an inset showing a structure element.

The ability to engineer the linear response of metamaterials to achieve exotic values of permittivity and permeability is well known, however their strong field localization also makes them very well suited to exhibiting exotic nonlinear phenomena. Previous work by our group has shown that individual split ring resonators can be made tunable and nonlinear by the introduction of diodes with voltage-controlled capacitance [4, 5], and that such resonators can be combined to create nonlinear metamaterial structures [6].

In this work, we demonstrate a nonlinear tunable metamaterial with a negative electric response. The structure is shown in Fig. 1, where two perpendicular sets of boards are introduced to create a relatively isotropic structure. Within each resonator, an additional gap is introduced where a varactor diode is placed, effectively having its capacitance in series with the capacitance of the resonator.

The sample is placed in a parallel plate waveguide, with a monopole source connected to a microwave amplifier in order to increase the output power available from the VNA. The transmission response is then measured as a function of the input power, and it is shown in Fig. 2(a). As there is significant ripple and some gain compression in the transmission response of the amplifier, the output of the amplifier is sampled using a directional coupler. The total transmission through the amplifier, waveguide, and metamaterial is then normalized to this quantity, which has largely eliminated artifacts due to the amplifier response.

It can be seen that our structure demonstrates two resonant stop bands within the measured frequency range. The lower band is due to currents flowing in opposite directions in each of the two rings of the resonator, as shown in Fig. 3(a). This results in two equal magnetic dipoles of opposite orientation, which have a zero net magnetic dipole moment (however, a significant magnetic quadrupole moment), and a dominant electric dipole moment due to the identical charge accumulation across each gap. Importantly, there is significant net current flowing through the central conductor containing the varactor diode. Thus we see that this resonant frequency is significantly modified by the incident power.

On the other hand, the higher frequency mode does not shift its frequency with a change of the incident power [see

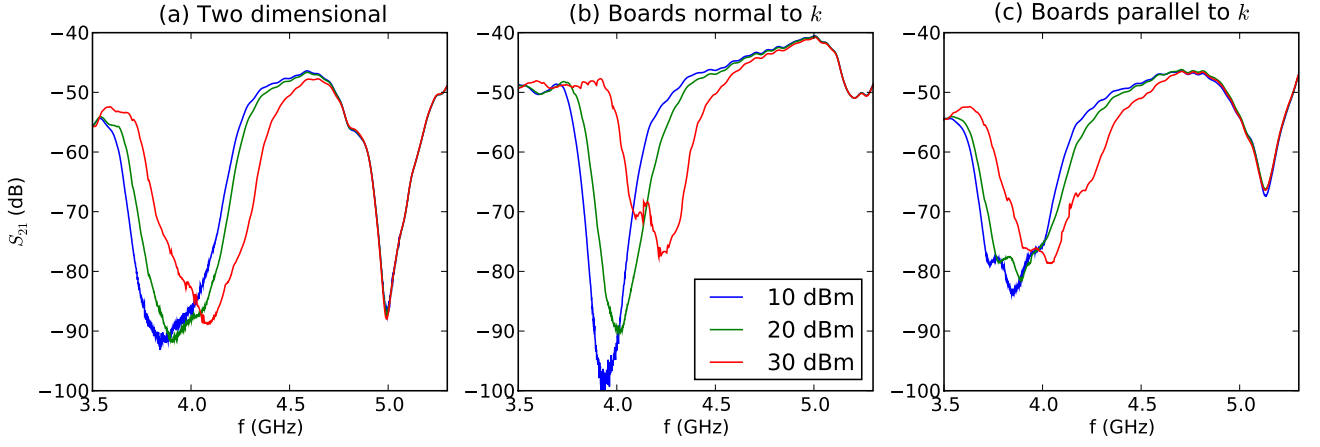


FIG. 2: Nonlinear transmission response.

Fig. 2(a)]. As can be seen in Fig. 3(b), this mode consists of two current loops in the same direction, thus resulting in a net magnetic dipole moment. As the accumulated charges across the gaps have opposite directions, this results in vanishing electric dipole moment, but nonzero electric quadrupole moment. As there is no net current through the central conductor, the nonlinear response of the varactor diode does not come into play. These mode configurations, and the stop-band locations, are in good agreement with numerical simulations performed in CST Microwave Studio [7].

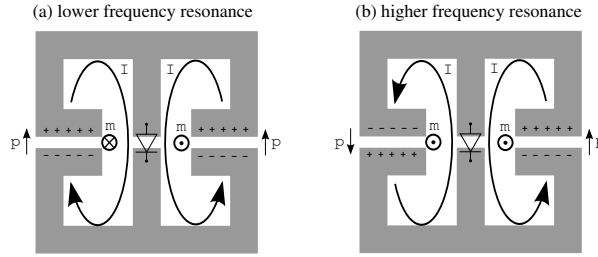


FIG. 3: Resonant modes of the electric resonators.

For comparison, we investigate the two different orientations of the circuit boards individually, i.e. those which are normal to the direction of propagation, and those which are parallel to it. The nonlinear transmission responses for these structures are shown in Figs. 2(b) and (c) respectively. In both cases a significant nonlinear response still occurs. In the case of the boards being perpendicular to the direction of propagation, the higher frequency magnetic stop-band does not exist. This is due to the symmetry of the fields across the gaps and the lack of any magnetic field component normal to the rings.

In conclusion, we have designed and analyzed, both numerically and experimentally, a nonlinear metamaterial with a dominant negative electric response. We expect that our results would allow to form the building blocks of a complete nonlinear negative-index metamaterial containing both nonlinear electric and magnetic elements.

- 
- [1] D. Smith, W. Padilla, D. Vier, S. Nemat-Nasser, S. Schultz, Phys. Rev. Lett. 84 (18) (2000) 4184–4187.
  - [2] R. Liu, A. Degiron, J. J. Mock, D. R. Smith, Appl. Phys. Lett. 90 (26) (2007) 263504.
  - [3] D. Schurig, J. J. Mock, D. R. Smith, Appl. Phys. Lett. 88 (4) (2006) 041109.
  - [4] I. Shadrivov, S. Morrison, Y. Kivshar, Opt. Express 14 (20) (2006) 9344–9349.
  - [5] D. A. Powell, I. V. Shadrivov, Y. S. Kivshar, M. V. Gorkunov, Appl. Phys. Lett. 91 (14) (2007) 144107.
  - [6] I. V. Shadrivov, A. B. Kozyrev, D. W. van der Weide, Y. S. Kivshar, Opt. Express 16 (25) (2008) 20266–20271.
  - [7] Computer Simulation Technology, <http://www.cst.com>.

# Hyperlens formed by array of metallic rods

**P.A. Belov<sup>1</sup>, G. Palikaras<sup>1</sup>, Y. Zhao<sup>1</sup> and C. Simovski<sup>2</sup>**

<sup>1</sup> Queen Mary University of London, London, UK,  
pavel.belov@elec.qmul.ac.uk, george.palikaras@elec.qmul.ac.uk, yan.zhao@elec.qmul.ac.uk  
<sup>2</sup> Helsinki University of Technology, Espoo, Finland,  
csimovsk@cc.hut.fi

A possibility to transfer electromagnetic field distributions with subwavelength resolution at microwave frequencies by means of parallel arrays of wires was proposed in [1]. The limitations of subwavelength imaging using such structures were analytically studied in [2], and experimental results aimed to verify the analytical findings were reported in [3].

Recently, motivated mainly by the limitations in the optical microscopy, there has been a growing interest in structures that are able to magnify subwavelength field distributions in the visible range [4-6]. This means that the details of the source distribution are retained while transferring the distribution over a certain distance, and at the same time the distribution is linearly magnified or enlarged. The capability of tapered arrays of wires to transmit, magnify and demagnify images with subwavelength details was demonstrated in [7]. However, the device proposed in [7] has spherical input and output interfaces which is not convenient for near-field imaging applications.

*In the paper we present first experimental results for hyperlens formed by tapered array of metallic wires.* In contrast to spherical geometry, the device contains wires with slightly different length. This limits imaging performance of the structure producing distortion of the image. However, the distortion is negligible provided that the maximum difference in between of the lengths of the wires is small.

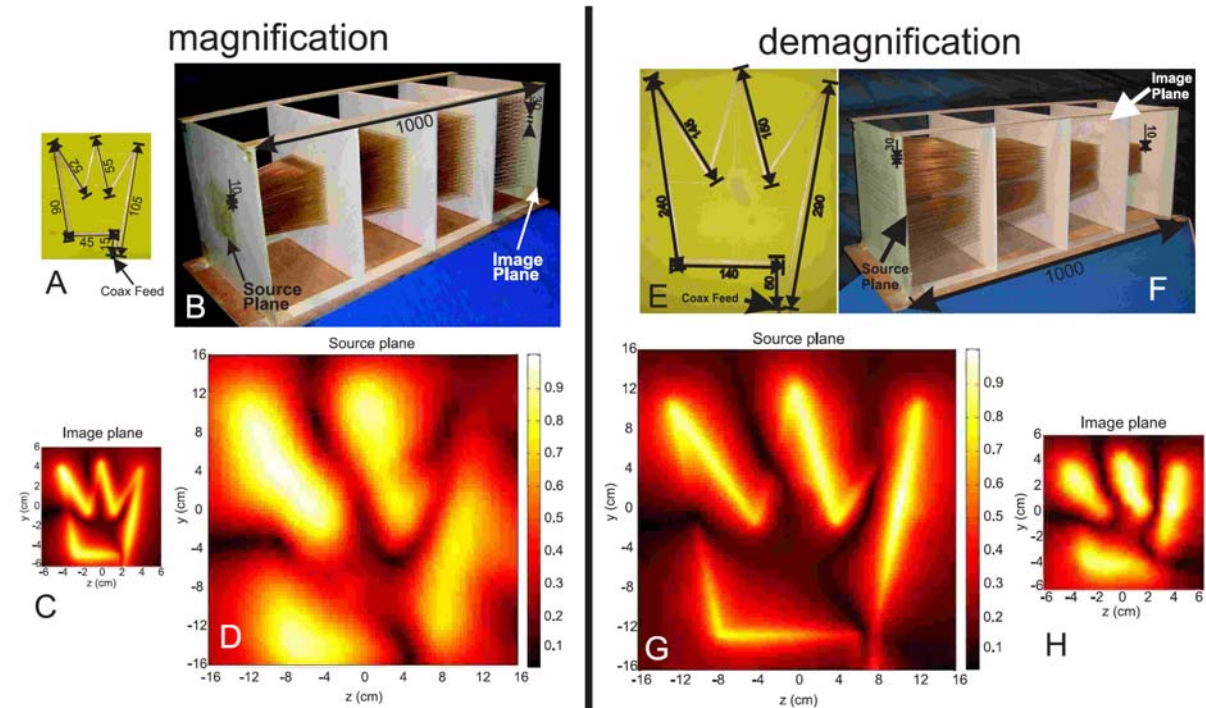
The magnifying lenses are expected to find immediate application in near-field microscopy as near-field to far-field transformers since they allow mapping field distributions with subwavelength details into images with details larger than the wavelength, which can be processed using conventional diffraction-limited imaging techniques. The demagnifying lenses allow creating complex near-field distributions on demand from their enlarged copies created in the far-field. On this route, it may be possible to create extremely compact near-field spots. The tapered wire medium lenses are especially attractive for application in the terahertz range [8]. In the microwave range the tapered wire medium endoscopes can be readily applied for the improvement of magnetic resonance imaging (MRI) systems and mechanical near-field microwave scanners.

The manufactured hyperlens (see Fig. 1.B) consists of copper wires whose separation is gradually enlarged. The slab is assembled as an array of 21x21 wires, with the lattice period being 5mm at the input interface and 15mm at the output. The source is a printed copper loop in the shape of a crown (see Fig. 1.A) fed by a coaxial cable. In the experiment, the planar crown-source was placed at 2 mm distance from the hyperlens input interface. The source field distribution was scanned over a planar surface located at a 2 mm distance behind the crown-source plane. The image field distribution is scanned over a planar surface located at a 7 mm distance behind the hyperlens output interface.

We have performed a series of measurements at several frequencies in the vicinity of 1050 MHz to identify the frequency that corresponds to the Fabry-Perot resonance (the electrical thickness of the slab in this frequency range is roughly 3.5 wavelengths). The best results correspond approximately to 1047 MHz (see Figs. 1.C,D), and at this frequency, the electrical length of the wires is about 3.49. A small deviation from the theoretical Fabry-Perot condition is most likely caused by the radially enlarging characteristic dimension of the slab. At the operational frequency, the source distribution is not affected by reflections, and the details of the distribution are canalized and simultaneously magnified across the slab. The crown shape (radial electric field component) is satisfactorily reproduced at the image plane, and the characteristic size of the pattern is magnified by a factor of 3.

The most interesting application of tapered arrays of wires is magnification of images with subwavelength resolution. However, the inverse operation is also possible. The tapered arrays are capable of demagnifying electromagnetic field distributions. This enables to obtain very tiny subwavelength distributions with any particular shape required for applications. In order to

demonstrate such a capability of tapered arrays of wires, we rotated the structure used in the magnification setup (Fig. 1.B) and interchanged source and image planes, see Fig. 1.F for details. We used a source in the form of a crown-shaped loop antenna (Fig. 1.E) which is approximately 3 times larger than one used in the magnification experiment. The source was placed in front of the larger interface of the slab and an excellent demagnified distribution has been created at the opposite interface. The results of the near-field scan are presented in Fig. 1.G,H. The distribution in the image plane reproduces all details of the source and appears to be three times smaller in size.



Setups and near-field measurement results for magnification and demagnification experiments. A,E) The crown-shaped near-field source used. B,F) The tapered array of wires. The source and image planes are marked by arrows. All dimensions are in mm. The distributions of electric field amplitude in C,G) source and D,H) image planes. The frequency of operation is 1047 MHz for magnification experiment and 455 MHz for demagnification experiment

## Conclusion

We have experimentally demonstrated the possibility of using dense arrays of metallic wires to magnify and demagnify images with a deeply sub-wavelength resolution and to transmit them to significant distances in terms of the wavelength. In particular, the transmission of an image with a  $\lambda/15$  resolution to an electrical distance that is as large as  $3.5 \lambda$  with triple magnification and with triple demagnification was experimentally shown. We anticipate that such near-field lenses may find applications in near-field microscopy and in medical imaging, starting from MRI systems that operate at low microwave frequencies and completing with a new generation of terahertz and infrared imaging devices. The proposed hyperlenses can be scaled down to micrometer scale for operation at terahertz and infrared frequencies [8].

P. Belov acknowledges financial support by EPSRC Advanced Research Fellowship EP/E053025/1.

## References

- <sup>1</sup> P.A. Belov, Y. Hao, and S. Sudhakaran, *Phys. Rev. B* **73**, pp. 033108 (1-4), 2006.
- <sup>2</sup> P.A. Belov, Y. Zhao, S. Sudhakaran, A. Alomainy, and Y. Hao, *Appl. Phys. Lett.* **89**, pp. 262109 (1-3), (2006).
- <sup>3</sup> P.A. Belov et al, *Phys. Rev. B* **77**, pp.193108 (1-4), (2008).
- <sup>4</sup> A. Salandrino and N. Engheta, *Phys. Rev. B* **74**, pp. 075103(1-5), (2006).
- <sup>5</sup> Z. Jacob, L. V. Alekseyev, and E. Narimanov *Optics Express* **14**, pp. 8247–8256, (2006).
- <sup>6</sup> Z. Liu, H. Lee, Y. Xiong, C. Sun, and X. Zhang, *Science* **315**, p. 1686 (2007).
- <sup>7</sup> P. Ikonen, C.R. Simovski, S. Tretyakov, P. Belov and Y. Hao, *Appl. Phys. Lett.* **91**, pp. 104102(1-3), (2007).
- <sup>8</sup> G. Shvets, S. Trendafilov, J.B. Pendry and A. Sarychev, *Phys. Rev. Lett.* **99**, pp.053903 (1-4), (2007).

# Soliton Mediated Optical Quantization in Bragg Gratings

Falk Eilenberger, C. Martijn de Sterke, and Benjamin J. Eggleton

CUDOS, School of Physics, University of Sydney, Sydney, NSW, Australia  
f.eilenberger@physics.usyd.edu.au

An intense pulse of light launched into the anomalous dispersion regime of a fibre typically undergoes a nonlinear evolution in which it splits into a discrete number of soliton pulses and a background of dispersive waves, which eventually radiate away from the solitons. The solitons themselves do not undergo dispersive broadening as they are stabilized by the nonlinearity [1].

We find experimentally and numerically that the interaction of the inherent discreteness of soliton propagation phenomena with the band structure of gratings manifests in the quantization of the transmission, which takes the form of a well-defined staircase (Fig. 1, 3). Each of the steps of the staircase is related to the transmission of a new soliton (Fig. 2, 4). For a given detuning, in the band gap, the transmission increases dramatically if the input power is large enough to create a new soliton.

Fibre-Bragg-Gratings (FBGs) written in the core of photosensitive fibres by means of exposure to an UV hologram are an excellent system to experimentally study this discretization behaviour of pulses close to and inside the band gap of those FBGs. As shown below, experimental data is in good agreement with numerical calculations based on nonlinear coupled mode equations.

This effect of Soliton Mediated Optical Quantization (SMOQ) has, to the best of our knowledge, not yet been discussed or observed in any systems and is unique to periodic structures and represents a new insight into the fundamental properties of nonlinear excitations of periodic media.

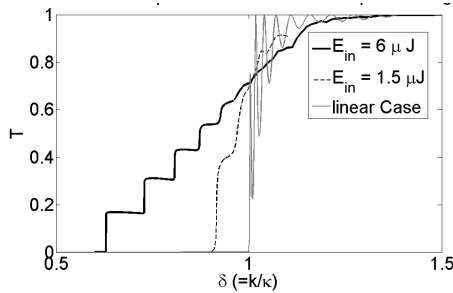


Fig 1. Simulated development of transmission staircase.  $L=100$  mm, apodized,  $\kappa=500\text{m}^{-1}$ , FWHM=700ps. (solid gray) Linear, cw. (dotted black)  $E=1.5 \mu\text{J}$ . (solid black)  $E=6 \mu\text{J}$ .

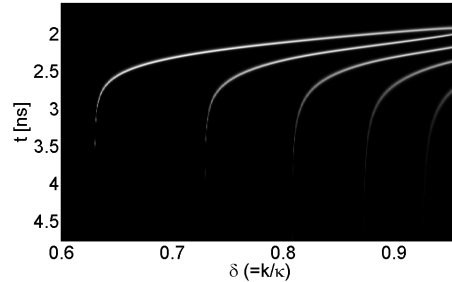


Fig 2. Simulated Time-resolved transmission spectrum. Each vertical slice depicts the temporal distribution of the optical power at the end of the FBG for a given detuning. Parameters as in Fig 1, solid black line

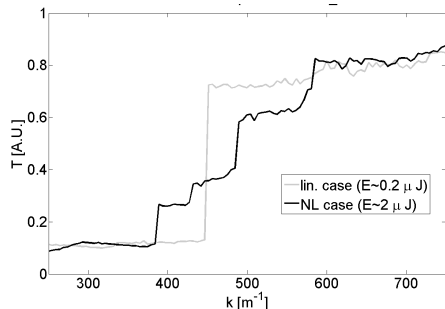


Fig 3. Experimental development of transmission staircase.  $L=90\text{mm}$ , apodized,  $\kappa=450\text{m}^{-1}$ , FWHM=700ps. (gray)  $E\sim 0.2 \mu\text{J}$ . (black)  $E\sim 2 \mu\text{J}$ ,

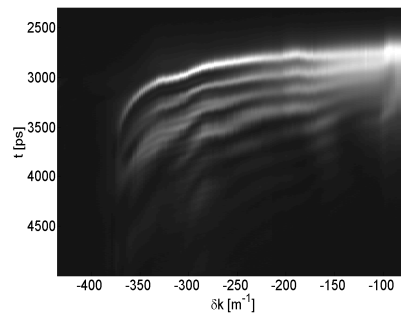


Fig 4. Time-resolved transmission spectrum. Each vertical slice depicts the temporal distribution of the optical power at the end of the FBG for a given detuning. Parameters as in Fig 3, black line.

## References

- <sup>1</sup> G. Agrawal, *Nonlinear Fibre Optics*, (2001).
- <sup>2</sup> H.G. Winful *et al.*, *Appl. Phys. Lett.* **35**, pp. 379-381, (1979).
- <sup>3</sup> W. Chen and D.L. Mills, *Phys. Rev. Lett.*, **58**, pp. 160-163 (1987)
- <sup>4</sup> J.T. Mok *et al.*, *Nature Phys.*, **11**, 770-775 (2006)